ELSEVIER

Ceramics International 25 (1999) 661–666

CERAMICS INTERNATIONAL

Methods of assessing gate solidification time in ceramic injection moulding

S. Krug[1], J.R.G. Evans*,[1]

Department of Materials Engineering, Brunel University, Uxbridge, Middlesex UB8 3PH, UK

Received 24 May 1998; received in revised form 25 June 1998; accepted 3 August 1998

Abstract

In ceramic injection moulding, the freezing of the gate separates the contents of the cavity from the barrel of the machine whereupon external control of the pressure on the solidifying moulding is lost. The gate freezing time can be deduced from analytical or numerical calculation, by reference to Heisler charts, by systematic studies of moulded mass as a function of time or by inference from the cavity pressure decay curve. In this work, a comparison is made between these methods and an experimental technique which allows the diameter of the molten channel to be measured directly as a function of time. It makes use of reverse extrusion of material and accommodates the influence of axial heat transfer from the heated nozzle of the machine. © 1999 Elsevier Science Ltd and Techna S.r.l. All rights reserved

Keywords: A. Injection moulding; Ceramic

1. Introduction

An unambiguous line of historical descent links ceramic injection moulding (1937) to polymer injection moulding (1872), to metal die casting (1849) and thence to the foundry processes of antiquity (ca. 3000 BC) [1]. In all these operations a liquid is fed into a cavity through a smaller channel where it solidifies to produce a shape. It follows that in each case the feeder channel solidifies before the contents of the cavity. This can give rise to shrinkage voids because of the higher thermal expansion coefficients of most liquids compared with their solids and because of the volumetric contraction on solidification. Such defects are found in sand casting [2] and exothermic feeders are sometimes used to prolong solidification. The problem can also occur in die casting and in the injection moulding of polymer composites [3]. In unfilled polymers, the shrinkage sometimes presents itself as surface ''sinking'' deformation because the low elastic modulus allows the solid layer to separate from the mould wall which in turn reduces the heat transfer coefficient [4]. In ceramic injection moulding the rigidity of the solid often prevents sinking deformation and encourages void formation [5,6].

The control of shrinkage during solidification therefore rests on methods of prolonging solidification of the feeder channels. These methods include the enlargement of the gate and runners, the use of hot runners [7], of insulated sprues [8], of modulated pressure [9], of reciprocating flow [10] or of open-ended moulding [11].

In the planning of such interventions it is helpful to know the natural solidification time of the runner and to compare it with that of the largest section of the moulding. The simplest approach is to consult Heisler charts for transient cooling in simple geometries [12]. Similarly, analytical or numerical methods can be used with a knowledge of heat transfer coefficient and enthalpy of solidification [4]. These methods neglect axial conduction, forced convective flow and the dependence of solidification temperature on pressure. They have a more serious weakness in the case of amorphous polymers which has been discussed in detail by Hunt [13]. The incidence of shrinkage voids is actually related to the inability of the feeding system to pack the mould and results from the imbalance of flow rate and volumetric shrinkage:

$$\left(\frac{dV}{dt}\right)_{\text{shrinkage}} \geqslant \left(\frac{dV}{dt}\right)_{\text{flow}}$$

* Corresponding author.

[1] Present address: Department of Materials, Queen Mary and Westfield College, Mile End Road, London, E1 4NS, UK.

0272-8842/99/$ - see front matter © 1999 Elsevier Science Ltd and Techna S.r.l. All rights reserved
PII: S0272-8842(98)00080-7

In the case of semicrystalline polymers, solidification occurs well above the glass transition temperature, T_g, at the crystalline solidification temperature, T_m, and viscosity rises steeply within about 10 K above T_m. The value of T_m, which is a material property, albeit subject to a slight pressure dependence, can often be used to deduce the freezing time for the runner axis. In the case of amorphous polymers the matter is not so simple. There is a steady increase in viscosity as T_g is approached and in that temperature regime the rate of moulding shrinkage may exceed the packing flow [13]. T_g is not therefore a reliable indicator of runner solidification.

In many cases, the cavity pressure trace gives the time at which the runner freezes. A steady pressure applied to the contents of the barrel registers on the cavity transducer up to the solidification time and thereafter falls. Interpretation of the cavity pressure trace is not always so straightforward. It records the pressure transmitted through the solidified wall of the moulding, acting on a freely sliding pin which activates a load cell embedded in the mould tool and its response is therefore related to the mechanical response of the solidified wall.

Systematic weighing of mouldings prepared under a fixed packing pressure for various times can also indicate the runner freezing time. Ideally the mass of the moulding increases until the runner freezes and is unchanged thereafter. Experimentally it relies on the mouldings being severed in exactly the same place each time a weighing is carried out.

2. Experimental methods

The ceramic injection moulding suspension [14], was composed of polyoxymethylene with 56 vol% ceramic (grade CT3000SG Alcoa Chemie GmbH, Ludwigshafen, Germany) prepared by high shear mixing and is commercially available as the grade Catamold A-OF from BASF (Ludwigshafen, Germany).

The mould cavity was a direct gated rectangular block 45×60×25 mm (Fig. 1). The mould tool was equipped with a pressure transducer located adjacent to the gate to prevent direct loading during injection as shown in Fig. 1. The injection moulding machine was a Negri-Bossi NB90 and was operated using the settings shown in Table 1. A Perkin–Elmer DSC2 differential scanning calorimeter was used to measure the solidification temperature at cooling rates of 1, 5 and 10°C/min.

3. Results and discussion

3.1. Cavity pressure

The cavity pressure as a function of time is shown in Fig. 2. The hold pressure in these experiments was varied from 40 to 100 MPa and was applied for 150 s. The graphs show that after the initial pressure peak which is caused by the injection pressure, a relatively constant cavity pressure is recorded until around 24–26 s after injection whereupon the pressure starts to drop. At high hold pressures, the inflection in the graphs is clear and distinct. In the time region between the injection peak and the pressure decay, almost constant cavity pressure prevails indicating a direct connection between the pressure applied by the screw and the liquid core of the moulding. When the sprue or gate freeze off the pressure supplied to the liquid core of the solidifying moulding is disconnected and the pressure in the isolated core decays. This method suggests a sprue solidification time of between 24 and 26 s for these moulding conditions.

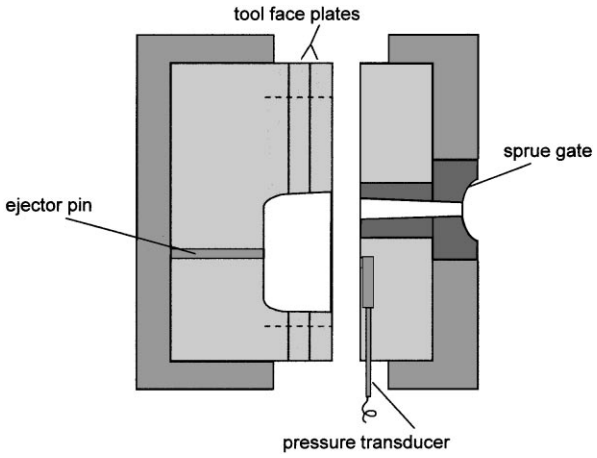

Fig. 1. Schematic diagram of the mould tool.

Table 1
Injection moulding conditions

Parameter	Setting
Barrel temperature profile	170–170–170–175°C (nozzle)
Mould temperature	135°C
Injection speed	8×10^{-5} m^3 s^{-1}
Hold pressure/time	80 MPa/150 s

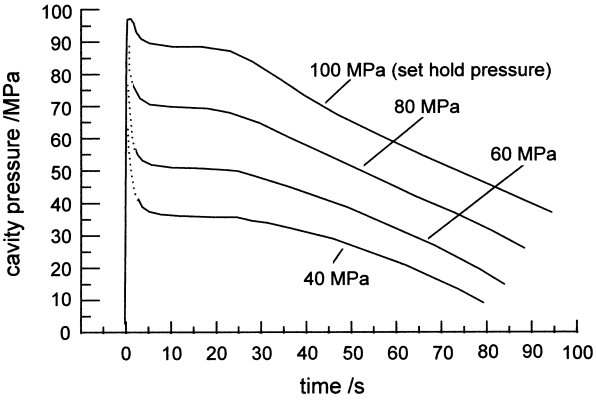

Fig. 2. Cavity pressure curves for different hold pressures.

3.2. Finite difference calculation

A finite difference program for an infinite cylinder was used to calculate the time required for the solidification of the centre of the sprue [4]. This treats the solidification of a cylinder of material having a diameter equivalent to the smallest end of the tapered sprue (10 mm). A fixed convective boundary condition was assumed with surface heat transfer coefficient 1000 $Wm^{-2}K^{-1}$. The data used for this calculation are given in Table 2. Fig. 3 shows the calculated cooling curve in the centre of a 10 mm cylinder in a mould tool at 130, 135 and 140°C. The melt is considered to solidify between 149 and 144°C. Peak temperatures of DSC solidification exotherms revealed an undercooling effect. While the melting endotherm peak (heated at 10°C/min) shows a maximum at 166°C, the solidification exotherms revealed different freezing peaks as a function of cooling rate, namely: 149°C at 1°C/min, 146°C at 5°C/min and 144°C at 10°C/min. These curves therefore predict the sprue to solidify at approximately 19, 23 and 31 s for mould temperatures of 130, 135 and 140°C, respectively, and for a 10°C/min cooling rate. In fact, the sprue cools somewhat faster but attempts to simulate this in the DSC leading to heat transfer induced errors. The actual mould temperature was 135°C and the predicted freeze-off time of 23 s matches well with the pressure drop recorded on the cavity pressure trace.

Table 2
Data used for numerical heat transfer calculations

Parameter	Value
Density	2700 $kg\,m^{-3}$
Thermal conductivity	1.55 $Wm^{-1}K^{-1}$
Specific heat	1029 $J\,kg^{-1}K^{-1}$
Radius	5 mm
Mould temperature	135°C
Melt temperature	175°C
Heat transfer coefficient	1000 $Wm^{-2}K^{-1}$

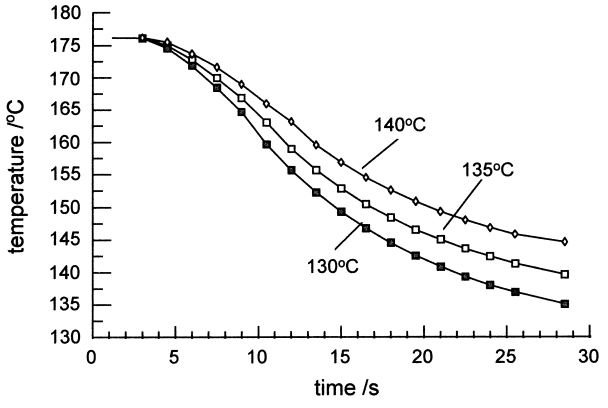

Fig. 3. Calculated cooling curves for the centre of an infinite cylinder of radius 5 mm in a mould at different mould temperatures.

Although such calculations give a fairly accurate guide to the freeze-off they fail to address the following factors.

i. In this calculation, the enthalpy of melting was neglected. This can easily be included [4] and produces a small increase in solidification time.
ii. The method neglects the forced convective flow of heat along the molten core of the cylinder during mould packing. This provides an additional heat source because the liquid flowing into the cavity to compensate for shrinkage has just been heated in the nozzle.
iii. The method neglects the axial conduction of heat from the heated nozzle. The smallest end of the conical sprue is selected for the calculation and this is the end most subject to axial heat flow.

These factors all tend to extend solidification and are sufficient to account for the disparity between the calculated solidification time and the cavity pressure decay curves.

3.3. Heisler charts

A simple method to estimate the gate solidification time is to use maps for the calculation of temperature distributions in simple geometric shapes. In Fig. 4 graphical plots of normalised centre temperature T, for an infinite cylinder, are shown for values of Biot's modulus, β, relevant for ceramic and metal injection mouldings where:

$$T = \frac{T_c - T_\infty}{T_i - T_\infty}, \beta = \frac{hR}{\lambda}, \tau = \frac{\alpha t}{R^2}$$

Here T_c is the centre temperature at time t, T_∞ is the centre temperature at infinite time, T_i is the initial temperature, h is the surface heat transfer coefficient, R the radius, λ the thermal conductivity and α the thermal diffusivity.

The calculated cooling time from the injection temperature of 175 to 144°C, which is taken as the solidification temperature at a cooling rate of 10°C/min, using the data in Table 2 gave a solidification time of 24 s. A slight error associated with graphical construction is present. The same reasons as those cited for numerical calculation may lead to a shorter predicted cooling time.

3.4. Gravimetric methods

This is an experimental method of assessing the gate solidification time which involves the production of a series of mouldings with different hold times. Since the solidification stage involves the progressive shrinkage of the moulding and its compensation by flow in the sprue

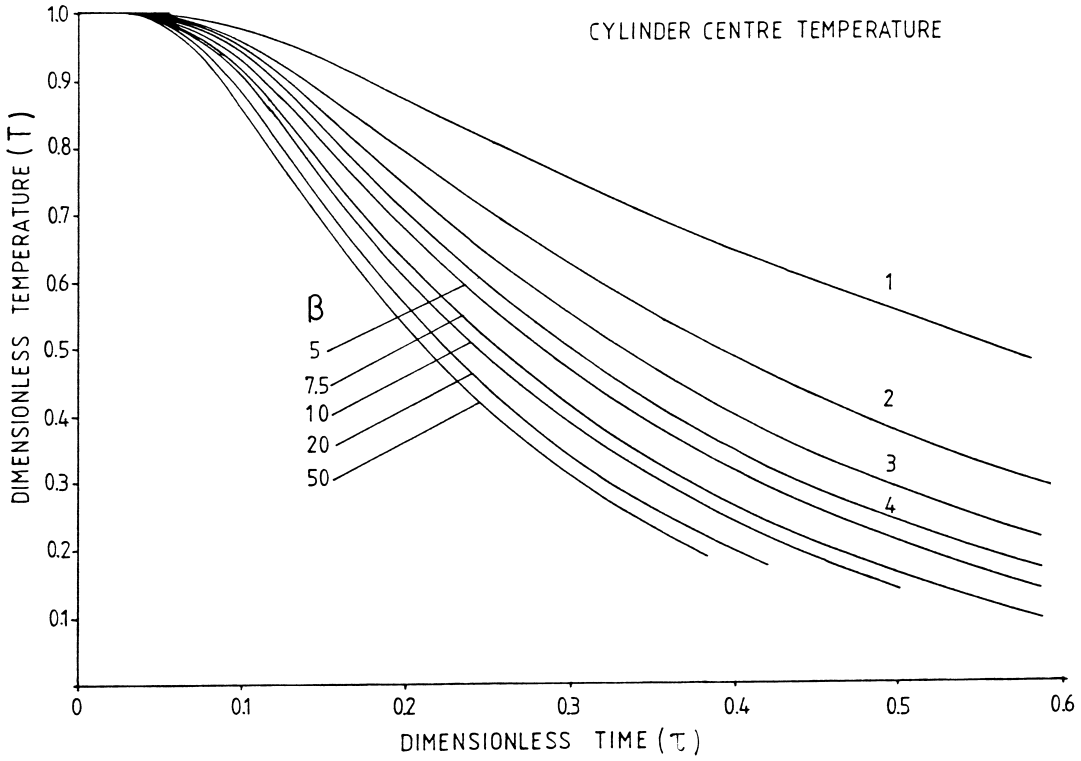

Fig. 4. Heisler chart for an infinite cylinder for values of Biot's modulus (β) relevant to ceramic moulding.

and runner, the mass of the moulding is expected to be a function of time until the gate freezes, whereupon it should remain unchanged. In the case of large section mouldings where the gate system freezes before the moulding is completely solidified, the final moulding weight is directly influenced by the sprue solidification time. Fig. 5 shows the moulding weight of 25 mm thick mouldings for different holding times and hold pressures. During the first 40 s of the packing stage, the hold pressure leads to an increase in moulding weight after which its influence is negligible. The sprue solidification time of approximately 40 s indicated here seems to exceed the predictions revealed by other methods.

The reason for this is that in the simple direct gating method used here the solidified sprue acts like a plunger on the partly solidified moulding. This means that the hold pressure still influences the final moulding weight even when the sprue is fully solidified. This is particularly the case at high hold pressures where the piston effect produces cracking around the gate. This might not be the case where a smaller gate was present between the sprue and the cavity. The design of runner chosen here was selected to give maximum passive solidification times.

3.5. Reverse extrusion method

A direct method can be used to estimate the solidification time of the sprue and to measure the diameter of the

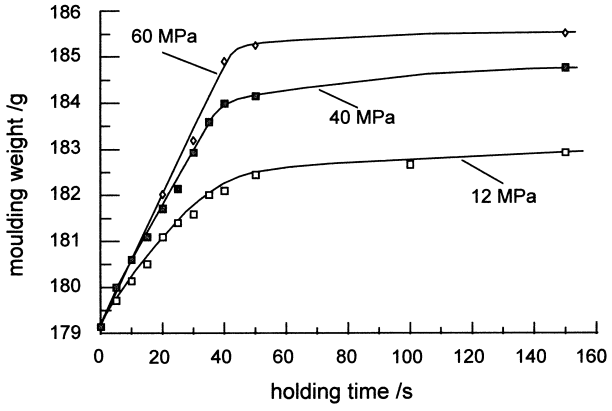

Fig. 5. Mass of mouldings as a function of hold time for different hold pressures.

molten core in the sprue throughout the solidification stage. This method makes use of the compressibility of the polymer melt. During conventional moulding, the nozzle stays abutted to the sprue until the mould is solidified. The injection-unit then travels back after the barrel has been redosed. To measure the actual molten core in the sprue, this sequence was changed. The injection-unit was set to move backwards immediately after the hold pressure stage had finished. If the hold pressure time was short, the core of the sprue was still molten. By using a high hold pressure (80 MPa for this experiment) the melt in the centre of the moulding was still in a state

of compression. If at this stage the carriage travels backwards and opens the sprue the melt expands and some material flows through the molten core out of the moulding where it can be seen and its diameter can be measured. Fig. 6 shows this reverse extrusion. The diameter of the extrudate shows the actual diameter of the remaining molten core in the sprue. A series of different hold pressure times was used in these experiments. Fig. 7 shows the measured diameter of the molten core as a function time.

With this relatively simple method it is possible to quantify the solidification progress of the sprue. Influences such as temperature gradients in the mould, the pressure decay during solidification, undercooling, the geometry of the sprue, axial heating effects from the nozzle and the effect of forced convection are all taken into account in this method. The graph shows a relatively uniform decay until at 20 s, a 5 mm molten core is left. It takes only another 6 s for the residual 5 mm to solidify. At 26 s after injection no flow through the sprue is possible. This direct experimental method agrees well with the solidification time deduced from the cavity pressure trace.

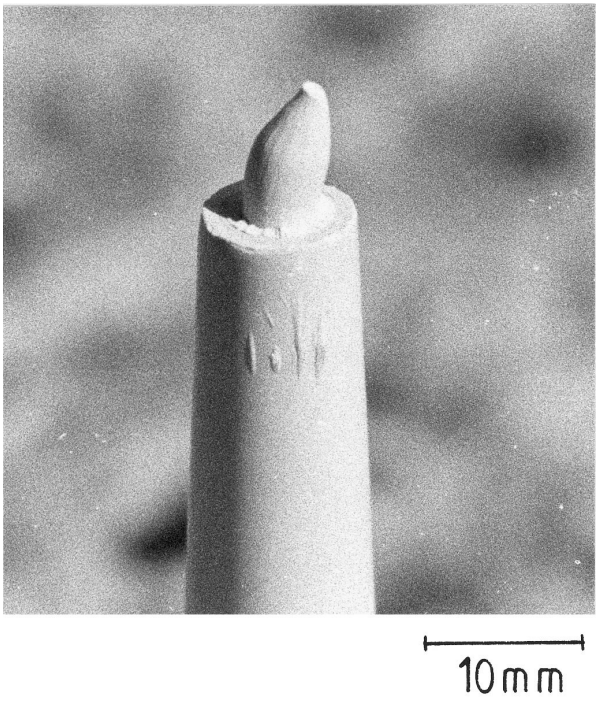

Fig. 6. Reverse extrusion from the sprue.

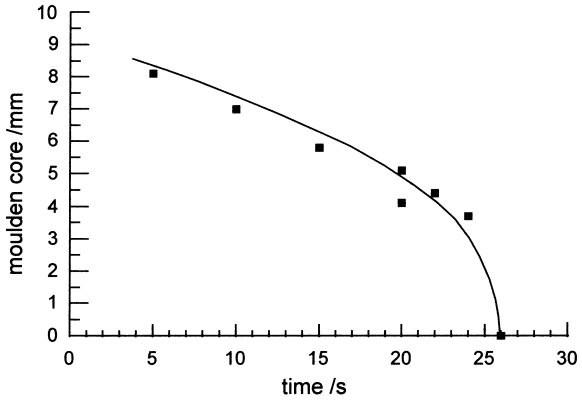

Fig. 7. Measured diameter of the molten core as a function of time.

4. Conclusions

Using identical moulding experiments, three experimental methods to assess runner solidification time were compared with each other and with theoretical calculations.

The method of detecting weight changes in mouldings was found to be very innaccurate because the runner arrangement allowed the fully solidified contents of the sprue to act as a piston. In contrast, good agreement was achieved between the numerical methods, the cavity pressure trace and a novel method of reverse extrusion. The latter allowed the diameter of the molten core to be recorded as a function of time up to solidification. The numerical methods gave slight underestimates of solidified time because they neglect, inter alia, axial heat flow and forced convection, both of which prolong solidification.

Acknowledgements

The authors are grateful to BASF (Ludwigshafen, Germany) for funding a studentship for one of us (S.K.) and to Mrs. K. Goddard for typing the manuscript.

References

[1] J.R.G. Evans, Injection moulding, in: R.J. Brook (Ed.), Materials Science and Technology, vol. 17A, VCH, Weinheim, 1996, pp. 267–311.
[2] G.J. Davies, Solidification and Casting, Applied Science Publishers, London, 1973, pp. 180–185.
[3] P.S. Allan, M.J. Bevis, The production of void-free thick section injection mouldings, Plast. Rubb. Proc. Appl. 3 (1983) 85–91.
[4] T. Zhang, J.R.G. Evans, The calculation of temperature distributions in ceramic injection moulding, J. Am. Ceram. Soc. 75 (1992) 2260–2267.
[5] T. Zhang, J.R.G. Evans, The solidification of large sections in ceramic injection moulding: I. Conventional moulding, J. Mater. Res. 8 (1993) 187–194.
[6] K.N. Hunt, J.R.G. Evans, J. Woodthorpe, Computer modelling of the origin of defects in ceramic injection moulding: II. Shrinkage voids, J. Mater. Sci. 26 (1991) 292–300.
[7] T. Zhang, J.R.G. Evans, The use of a heated sprue in the injection moulding of large ceramic sections, Br. Ceram. Trans. J. 92 (1993) 146–151.

[8] S. Krug, J.R.G. Evans, J.H.H. ter Maat, J. Am. Ceram. Soc., in press.
[9] J.G. Zhang, M.J. Edirisinghe, J.R.G. Evans, The use of modulated pressure in ceramic injection moulding, J. Eur. Ceram. Soc. 5 (1989) 63–72.
[10] T. Zhang, J.R.G. Evans, M.J. Bevis, Control of fibre orientation in injection moulded ceramic composites, Composites A28 (1997) 339–346.
[11] T. Zhang, J.R.G. Evans, M.J. Bevis, The control of fibre orientation in ceramic and metal composites by open-ended injection moulding, Comp. Sci. Technol. 56 (1996) 921–928.
[12] M.P. Heisler, Temperature charts for induction and constant temperature heating, Trans. ASME 69 (1947) 227–236.
[13] K.N. Hunt, J.R.G. Evans, J. Woodthorpe, Computer modelling of the origin of defects in ceramic injection moulding: III. Sprue closure, J. Mater. Sci. 26 (1991) 2143–2149.
[14] J.H.H. ter Maat, J. Ebenhoech, Feedstocks for ceramic injection moulding using the catalytic debinding process, in: P. Duran, J.F. Fernandez (Eds.), Proc. 3rd Congr. Euro. Ceram. Soc, Madrid, Faenza Editrice Iberica, Castellon, Spain, 1993, pp. 437–443.